14th International Conference on Structural Safety and Reliability - ICOSSAR'25
1-6 June, 2025 - Los Angeles California, USA
R. Ghanem, E. Johnson, S. Masri and A. Olivier (Eds)

BRIDGING DATA GAPS IN FRAGILITY MODELING FOR COASTAL INFRASTRUCTURE RESILIENCE

NARGES SAEEDNEJAD[1] **and JAMIE ELLEN PADGETT**[1,2]

[1] Department of Civil and Environmental Engineering, Rice University
Houston, TX, USA

[2] Ken Kennedy Institute, Rice University
Houston, TX, USA
Email (corresponding): Narges.saeednejad@rice.edu

Key words: Fragility models, Bayesian updating, Transfer learning, Hurricane-induced damage, Structural reliability

Abstract. Coastal infrastructure is highly exposed to hurricanes and severe storms, underscoring the need for reliable fragility models that predict structural performance under extreme hazards. Over the past fifty years, methodologies for generating and validating building fragility curves have advanced considerably, but calibration and validation continue to lag due to scarce damage records and domain-specific assumptions. While numerical and simulation-based frameworks exist for single- and multi-hazard scenarios, they may lack transferability and robust empirical verification. Machine learning techniques present opportunities to overcome these limitations by enabling adaptive, continually evolving fragility functions. We propose a methodology integrating conventional transfer learning and hierarchical Bayesian transfer learning to enhance model flexibility and precision, especially in data-scarce coastal regions. This approach refines existing simulation- or data-rich region-derived models with limited labeled damage data from new target areas, improving predictive accuracy and closing the gap between theoretical simulations and observed outcomes. We demonstrate its feasibility through residential building case studies impacted by Hurricane Ian. By leveraging both physical simulations and sparse field observations, the framework supports ongoing model learning and adaptation. By delivering more accurate, region-specific fragility assessments, this framework advances vulnerability analysis and supports resilient coastal infrastructure planning.

1 Introduction

Coastal communities in the United States face significant hurricane risk, with a large segment of the population residing within roughly 80 km of the shoreline [1]. Projections indicate that this coastal population will continue to grow in both density and geographic extent [2], and although some studies suggest a decline in overall tropical storm frequency, the storms that do occur are expected to be more intense [3]. In this context, robust fragility models—which estimate the conditional probability of a structure reaching or exceeding a specified damage state given a hazard intensity measure—are essential [4], [5]. These curves can be derived from empirical damage records, physics-based simulations, or expert judgment, and over the past fifty years methodologies for generating and validating building

fragility models have advanced considerably [6], [7], [8], [9]. However, empirical approaches remain constrained by limited historical data for extreme events, while simulation-based models often target specific structural archetypes and may lack comprehensive validation against real-world observations [10]. Machine learning (ML) techniques have been explored in structural design and performance assessment since at least the late 1980s—Adeli and Yeh pioneered an ML-based beam design method in 1989 [11]—and more recent applications include post-hurricane damage analysis [12], [13], [14] and near-real-time damage detection via social media streams [15], [16]. Although these ML tools have improved recovery operations, they are less suited for pre-event risk analysis, and ML-driven damage estimation models remain relatively uncommon with moderate predictive skill. At the regional scale, a random-forest regression of environmental and social variables explained only 29% of the variance in damage for Hurricane Maria [17], while Wendler applied eight ML algorithms to wind-only metrics and achieved R^2 values of 0.50–0.60 [18]. At the building level, a Bayesian network combining surge simulations and engineering theory classified Hurricane Sandy damage with accuracies of 68.4%, 95.8%, 4.4%, and 0% for "affected," "minor," "major," and "destroyed" states, respectively [19], and a proportional-odds logit model predicted three damage levels for Katrina-impacted buildings with 84% accuracy [9]. Klepac et al. [20] introduced a data-driven framework that integrates building, hazard, and geospatial features in a random forest to hindcast damage from Hurricanes Harvey, Irma, Michael, and Laura with 76% accuracy. Building upon these foundations, the present study integrates transfer learning and Bayesian updating to develop fragility models that are both flexible and precise for coastal infrastructure. By refining existing simulation-based models with limited, locally labeled damage data, our methodology bridges the gap between theoretical models and observed outcomes. We demonstrate this approach through a case study of residential buildings impacted by Hurricane Ian, aiming to enhance vulnerability assessments and support more resilient coastal infrastructure planning.

2 Methodology

This paper investigates and compares distinct approaches for developing hurricane fragility models tailored to a specific target region, particularly addressing the common challenge of limited local damage data. The core strategy involves leveraging knowledge from an existing, pre-established "base" fragility model, which represents prior understanding derived from broader data or simulations. Two primary paradigms are explored for adapting this base knowledge to the target region: conventional Transfer Learning (TL) and Hierarchical Bayesian Transfer Learning (HBTL).The TL approaches involve fine-tuning the base model parameters and potentially incorporating additional local features (e.g., building age, shoreline distance, area) using optimization techniques applied to the target data. In contrast, the Hierarchical Bayesian Transfer Learning (HBTL) framework offers a probabilistic paradigm for knowledge adaptation. It leverages the Bayesian principle where prior beliefs about model parameters, informed by the source domain (the base model), are updated based on the target domain data. The subsequent sections detail the specific base model adopted, describe the target region dataset, and elaborate on the implementation and evaluation of these distinct modeling scenarios.

2.1 Base Fragility Model

This study adopts the multi-hazard fragility framework developed by Do. et al. [21] as its baseline, chosen for its explicit accounting of combined storm surge and wave loads on residential build-

ings.The reference model provides fragility functions specifically derived for wood-framed, single-story residential buildings, parameterized according to distinct First Floor Elevation (FFE) categories. As a result, every FFE category considered here is represented by its own set of statistically derived fragility coefficients from the Do et al. methodology.

The functional form of the base fragility model, representing the probability of failure (P_f) as a function of surge depth (d) and wave height (w), is given by:

$$P_f(d, w) = \frac{Z(d, w)^\beta}{Z(d, w)^\beta + 1} \tag{1}$$

where $Z(d, w)$ represents a combined hazard index defined as:

$$Z(d, w) = \frac{d}{A} + \frac{w}{B} + C\left(\frac{d}{A}\right)\left(\frac{w}{B}\right) \tag{2}$$

The parameters $A, B, C,$ and β are the fragility coefficients specific to each FFE category, whose values are adopted from the reference study. Do et al.'s methodology uses high-fidelity 3D CFD in ANSYS Fluent—validated against both laboratory wave-flume tests and full-scale/scale-model experiments—to generate component pressure responses under combined surge and wave loads. These responses are then processed via Monte Carlo simulations to produce surge-and-wave fragility functions. The resulting fragility surfaces have demonstrated applicability in vulnerability assessments for residential buildings in coastal areas, such as Galveston, TX.

2.2 Feature Selection for Extended Models

While the foundational fragility model relies solely on hazard intensity measures and first floor elevation, incorporating additional building-specific characteristics available in the target region—such as building age, distance to shoreline, and footprint area—has the potential to enhance the model's predictive accuracy by capturing local vulnerabilities not present in the source data used for pre-training. A systematic feature-selection step is performed before running the transfer-learning scenarios with extended inputs. Every possible subset of these standardized candidate features was evaluated via K-fold cross-validation within each First-Floor Elevation (FFE) category. We then aggregated each subset's performance across FFEs using a sample-weighted average of the F1 score—which fairly represents the model's ability to correctly identify both failures and non-failures. The feature subset achieving the highest weighted F1 score was adopted for the extended-feature transfer-learning runs, ensuring we leverage the most informative local data while maintaining model parsimony. As shown in (fig.1), the combination of building age and distance to shoreline ("Age, Dist") achieved the highest overall weighted F1 score (0.682).

The extended fragility model is as below:

$$Z_{ext}(d, w, x_{age}, x_{dist}, x_{area}) = Z(d, w) + \gamma_{age} \cdot x_{age} + \delta_{dist} \cdot x_{dist} + \epsilon_{area} \cdot x_{area} \tag{3}$$

where $Z(d, w)$ is the original hazard index from Equation 2, and $\gamma_{age}, \delta_{dist}, \epsilon_{area}$ are the parameters corresponding to the standardized age, distance, and area features, respectively. These parameters represent the sensitivity of the combined hazard index to variations in the respective building characteristics. Note that the specific parameters included depend on the outcome of the feature selection process; Equation 3 shows the case where all three features were selected.

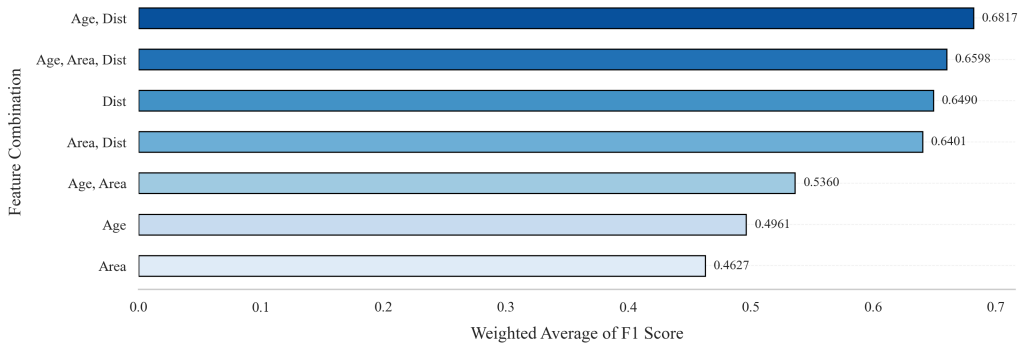

Figure 1: Weighted average F1 score across all FFE categories for each candidate feature subset.

The probability of failure, P_f, for the extended model retains the same functional form as the base model, but utilizes the extended hazard index Z_{ext}:

$$P_f(d, w, x_{age}, \dots) = \frac{Z_{ext}^{\beta}}{Z_{ext}^{\beta} + 1} \tag{4}$$

where β is the same shape parameter as in the base model.

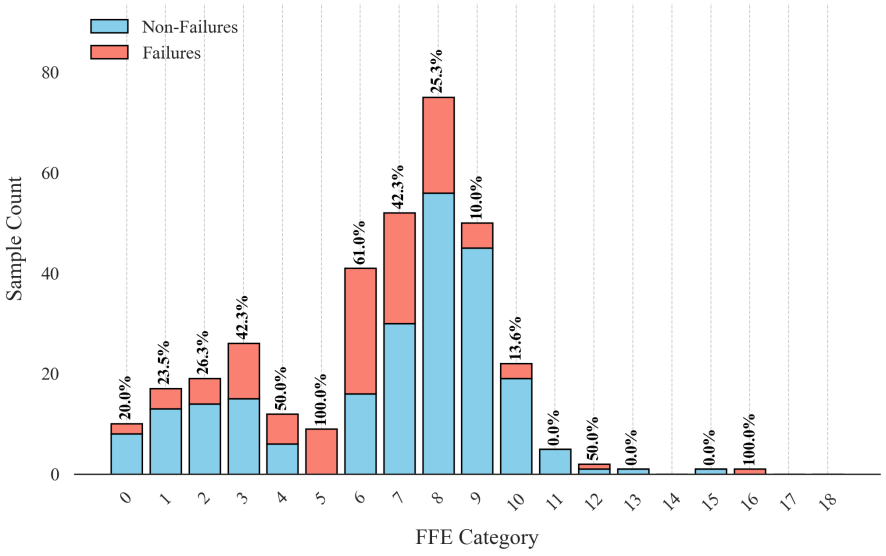

Figure 2: Stacked bar chart of non-failures (blue) and failures (red) across First-Floor Elevation (FFE) categories in the Fort Myers dataset, with percentages above each bar indicating the proportion of failures within that category.

2.3 Target Region

To evaluate the performance of the proposed methodologies, this study utilizes a dataset documenting damage to residential buildings in Fort Myers, Florida, following Hurricane Ian [22, 23].The referenced dataset correlates observed damage states with the corresponding hazard intensity measures, surge depth and wave height, experienced during Hurricane Ian. Although the full spectrum of damage states is available, here we apply our method to the final damage state—complete structural

failure—since the same procedure can be repeated to model intermediate damage levels. To align with the scope of the base fragility model, our analysis is limited to single-story, wood-framed residences. Furthermore, consistent with the categorization inherent in the base model, the observed building damage data within the target region (Fort Myers) was stratified into 19 distinct categories based on the First Floor Elevation (FFE) of the buildings. This FFE-based categorization inherently resulted in subsets with limited or no data points for certain categories. Moreover, it introduced significant class imbalance within several FFE categories, as the proportion of damaged versus undamaged buildings varied considerably depending on the elevation and experienced hazard intensity. Hazard intensities including wave height and surge depth were derived from ADCIRC and SWAN hindcast simulations for this study [24]. The distribution of samples and the failure percentages across the primary FFE categories are illustrated in (fig.2). To ensure robustness of the analysis, FFE categories containing fewer than 10 total data points (combining both failure and non-failure observations) were excluded from subsequent modeling and evaluation phases.

2.4 Conventional Transfer Learning

The conventional Transfer Learning (TL) approach implemented in this study adapts the pre-established base fragility model parameters (A, B, C, β) to the target region data using optimization. Parameter fine-tuning is achieved by minimizing an objective function comprising a weighted binary cross-entropy loss term and L2 regularization penalties, utilizing the L-BFGS-B algorithm. The weighted cross-entropy addresses potential class imbalance in the target dataset by assigning higher weights to the minority class, calculated based on inverse class frequency within the training subset. L2 regularization is applied distinctly: base parameters (A, B, C, β) are penalized for deviating from their original pre-trained values (θ^*_{base}), while any incorporated extended parameters (γ_j, corresponding to features like standardized age, distance, or area) are penalized for deviating from zero. The objective function is thus:

$$\mathcal{L}_{total} = \mathcal{L}_{CE\_weighted} + \frac{\lambda_{base}}{2}||\theta_{base} - \theta^*_{base}||_2^2 + \frac{\lambda_{ext}}{2}||\theta_{ext}||_2^2 \tag{5}$$

The regularization strengths ($\lambda_{base}, \lambda_{ext}$) are determined through hyperparameter optimization via grid search and stratified K-fold cross-validation in FFE categories with sufficient and more balanced data, and Leave-One-Out cross-validation for FFE categories with limited data , selecting the values that yield the best performance on a chosen metric. Extended features, when included based on the feature selection outcome, modify the hazard index using an additive approach ($Z_{ext} = Z_{base} + \sum \gamma_j x_j$). The TL scenarios explored include adapting only base parameters, or adapting both base and selected extended parameters.

2.4.1 Evaluation Scenarios

To systematically evaluate the effectiveness of various adaptation strategies, several distinct scenarios were designed and implemented:

1. **Target Only:** This scenario serves as a lower benchmark. It involves training a fragility model using only the limited target data available for each building category (FFE), without leveraging any information from the pre-trained base model. It uses only the core hazard features (surge depth and wave height).

2. **Base Model Evaluation:** This scenario represents the performance of the pre-trained fragility model when applied directly to the target region without any adaptation or retraining. It provides a reference point to assess the necessity and benefit of adaptation.

3. **Transfer Learning (TL) - Base Features:** This is a standard TL approach where the pre-trained base model parameters (A, B, C, β) are used as a starting point and then fine-tuned using the target data. Only the core hazard features are used, and all four base parameters are adapted during optimization.

4. **TL - Extended Base Model:** This scenario builds upon standard TL by incorporating the optimally selected subset of extended features (e.g., standardized age, distance, area) identified during the feature selection phase. Both the base parameters (A, B, C, β) and the parameters associated with the selected extended features (γ_j) are simultaneously adapted using the target data.

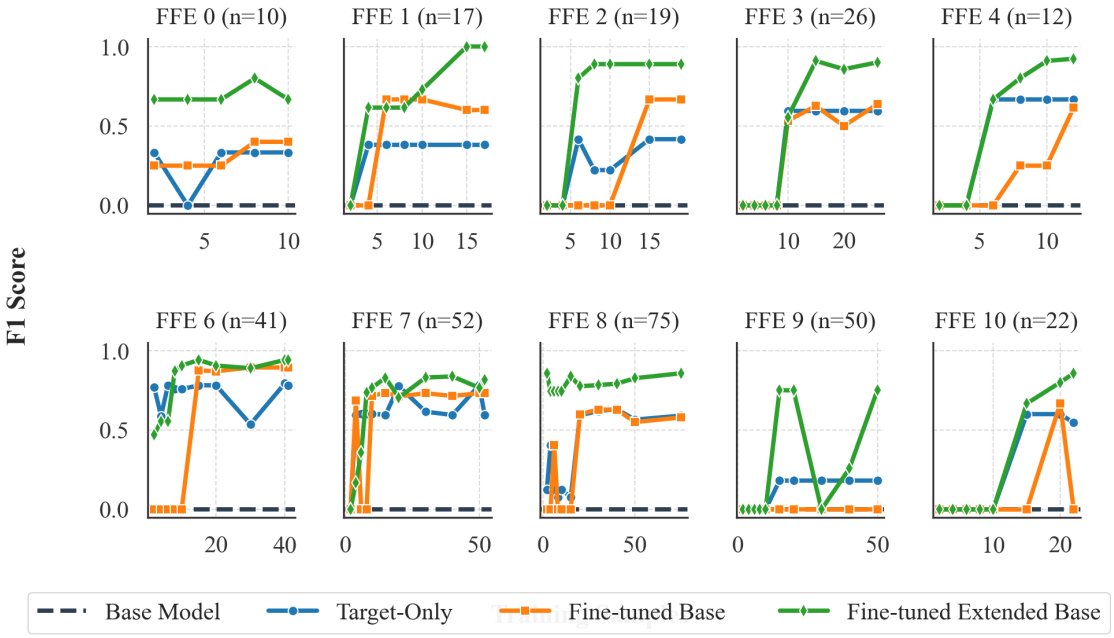

Figure 3: Incremental F1-score as a function of target training sample size across FFE categories.

2.4.2 Sensitivity of Transfer-Learning Performance to Target Sample Size

As shown in (fig.3), the unadapted base model yields near-zero F1 scores across all FFEs, while the target-only model gradually improves to about 0.4 with 10–20 samples. Fine-tuning the base parameters produces a much steeper rise—achieving 0.6–0.8 F1 with only 5–10 samples—and incorporating the selected extended features further boosts performance, often exceeding 0.8–1.0 in well-sampled categories. However, the curves also reveal a clear sensitivity to the number of target samples: in categories with fewer than 5–10 observations (e.g., FFE 0 and FFE 9–10), all models struggle, showing erratic or flat F1 gains. Beyond roughly 10–15 samples per FFE, performance

plateaus for most categories, indicating diminishing returns from additional data. This underscores that while transfer learning—even with minimal data—can rapidly improve predictive accuracy, there remains a practical lower bound on sample size below which model reliability cannot be guaranteed.

2.5 Hierarchical Bayesian Transfer Learning

Transfer learning is a data-driven approach wherein a model trained on a data-rich source domain is adapted for use in a data-scarce target domain. The key idea is to reuse the knowledge learned from the source domain (for example, extensive simulation data or historical failure data) and fine-tune the model with the limited data available in the target domain. In the Bayesian context, this knowledge transfer is achieved by using information from the source domain to inform the prior distributions for the target domain model. To address the potential data scarcity within individual First Floor Elevation (FFE) categories and to formally incorporate prior knowledge from existing base fragility models, a Hierarchical Bayesian Model (HBM) was developed in this step. This approach allows for information pooling across different FFE categories, where estimates for data-sparse categories can borrow strength from data-rich categories, while simultaneously providing a principled framework for uncertainty quantification. This specific HBM focuses on estimating the four core parameters of the base fragility model (A, B, C, β).

The model assumes that for each FFE category, the parameters $\{\theta_{ffe} = \{A_{ffe}, B_{ffe}, C_{ffe}, \beta_{ffe}\}\}$ are drawn from common distributions governed by hyperpriors. The probability of damage $P_{f,i}$ for observation i in category $ffe[i]$ is modeled using a sigmoid function applied to the log-transformed combined hazard index Z_i:

$$P_{f,i} = \text{sigmoid}(\beta_{ffe[i]} \cdot \ln(Z_i)) \tag{6}$$

$$Z_i = \frac{d_i}{A_{ffe[i]}} + \frac{w_i}{B_{ffe[i]}} + C_{ffe[i]} \left(\frac{d_i}{A_{ffe[i]}}\right) \left(\frac{w_i}{B_{ffe[i]}}\right) \tag{7}$$

where d_i and w_i are the surge depth and wave height, respectively. Parameters A, B, C, and β are constrained to be positive. The sigmoid function is defined as $\text{sigmoid}(x) = 1/(1 + e^{-x})$.

2.5.1 Prior Specification

One of the central elements of the hierarchical Bayesian model (HBM) is the specification of priors and hyperpriors to transfer domain knowledge from the base fragility model into each First-Floor Elevation (FFE) category:

- **Hyperpriors on means (μ_p):** We place normal hyperpriors on μ_A, μ_B, μ_C, and μ_β, each centered at the corresponding average value from the base model. To enforce positivity for A and C, μ_A and μ_C are specified on the log scale, i.e., as log-normal priors.
- **Hyperpriors on standard deviations (σ_p):** We assign half-normal hyperpriors to σ_A, σ_B, σ_C, and σ_β, representing uncertainty in parameter variability around their means.

$$\{A_{\text{ffe}},\ B_{\text{ffe}},\ C_{\text{ffe}},\ \beta_{\text{ffe}}\}$$

  - **FFE-specific parameters:** For each elevation category:
    - $A_{\text{ffe}} \sim \text{LogNormal}(\mu_A, \sigma_A)$

* $B_{\text{ffe}} \sim \mathcal{N}(\mu_B, \sigma_B)$
* $C_{\text{ffe}} \sim \text{LogNormal}(\mu_C, \sigma_C)$
* $\beta_{\text{ffe}} \sim \mathcal{N}(\mu_\beta, \sigma_\beta)$

This hierarchical structure implements Bayesian transfer learning by allowing base-model-derived hyperpriors to inform parameter estimates in data-scarce FFEs.

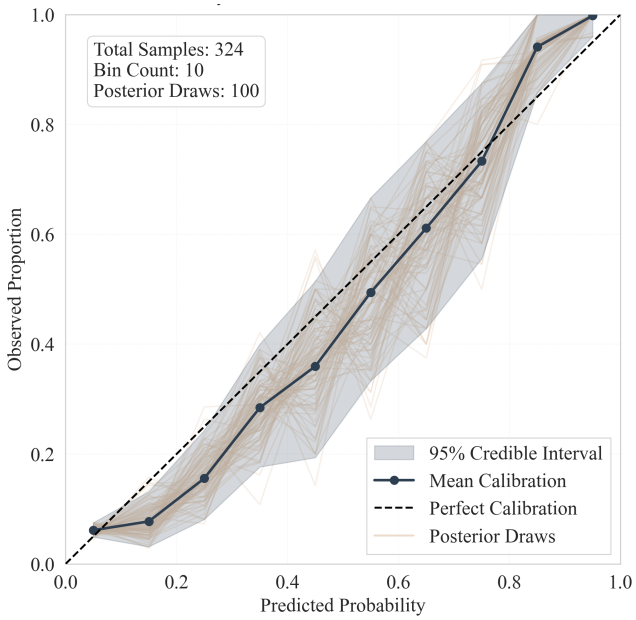

Figure 4: Bayesian calibration plot comparing predicted probabilities to observed frequencies.

2.5.2 Likelihood and Class Imbalance Handling

The likelihood of observing the binary damage outcome y_i (0 or 1) given the predicted probability $p_{f,i}$ is modeled using a Bernoulli distribution:

$$y_i \sim \text{Bernoulli}(p_{f,i}) \tag{8}$$

To account for class imbalance, a weighted likelihood formulation is used. Each observation's contribution to the log-likelihood is scaled by a weight w_i:

$$\log(\mathcal{L}_{weighted}) = \sum_i w_i \log(\text{Bernoulli}(y_i|p_{f,i})) \tag{9}$$

The weights w_i are derived from the scaled inverse frequency of its class ($\propto \sqrt{N_{total}/N_{class(i)}}$), emphasizing the minority (damaged) class during inference.

2.5.3 Model Inference

Parameter estimation is performed via Markov Chain Monte Carlo (MCMC) using the No-U-Turn Sampler (NUTS). Posterior distributions provide estimates of the parameters for each FFE category

along with their associated uncertainty. Convergence is assessed using standard MCMC diagnostics ($\hat{R}$, ESS). Prior predictive checks were also performed. As shown in (Fig. 4), the Bayesian calibration curve—with individual posterior draw trajectories, the 95% credible band, and the mean calibration line—closely tracks the 45° ideal, demonstrating that the posterior predictive probabilities align well with observed frequencies across probability bins.

2.5.4 Model Evaluation

As shown in (fig.5) the Bayesian-posterior prediction intervals are grouped by First Floor Elevation (FFE) category. In each panel, the solid line is the median predicted probability, the shaded band is the 95% credible interval from the posterior draws, and the semi-transparent markers at the top and bottom show the observed damage outcomes (1 = failure, 0 = no failure). The dashed red line at 0.5 marks the classification threshold. Lower-data FFEs (e.g., FFE 0 and FFE 9–10) exhibit wider intervals and median curves near zero, indicating greater uncertainty, whereas well-sampled FFEs (e.g., FFE 2–5) show narrower bands and smoothly rising medians, reflecting increased confidence.

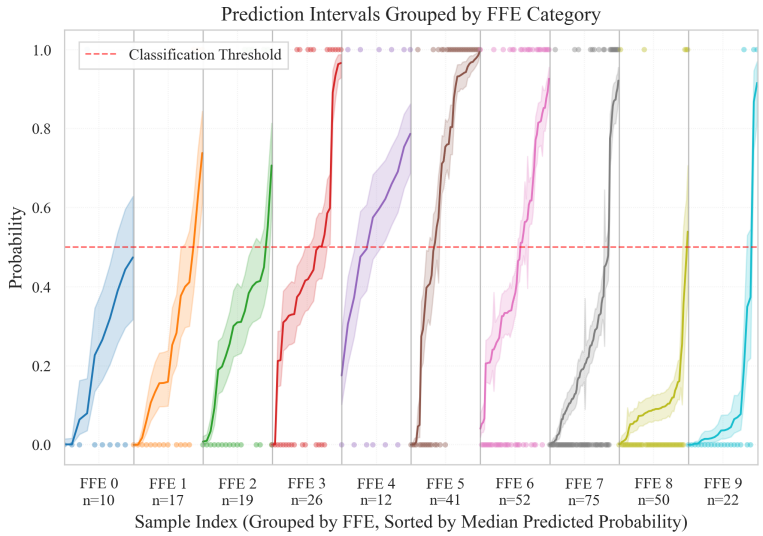

Figure 5: Prediction intervals grouped by FFE category. Each panel shows median predictions (solid), 95% credible intervals (shaded), and observed outcomes (dots), with the 0.5 classification threshold (dashed).

(fig. 6) presents the same intervals pooled across all FFEs and sorted by the median predicted probability. The overall 95% credible band and median curve provide a global view of uncertainty and discrimination: observed failures cluster at high probability indices, while non-failures lie at the low end, demonstrating the model's ability to rank buildings by risk.

3 Discussion

The methodology presented in this paper offers a clear pathway to bridge the gap between high-fidelity, simulation-based fragility curves and the reality of limited, noisy post-hurricane damage data. By adopting Do et al.'s surge–and-wave fragility model as a principled "base," the study first shows how conventional transfer learning can rapidly recalibrate the core parameters (A, B, C, β) to new regional data—especially once just a handful of target buildings (10 samples per FFE) are

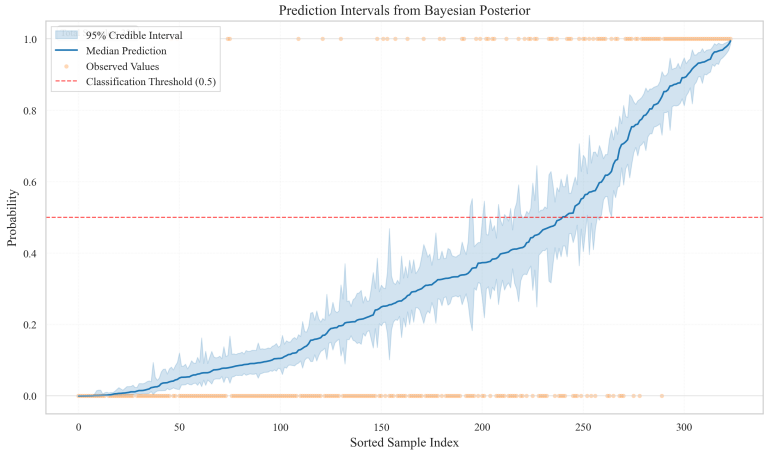

Figure 6: Prediction intervals for all samples sorted by median predicted probability.

available—and how chosen additional features (age, shoreline distance, footprint) can further boost point-estimate accuracy. It then demonstrates that a hierarchical Bayesian transfer-learning framework not only pools information across sparsely populated elevation bins (thereby stabilizing estimates in the most data-scarce categories) but also yields full posterior distributions, producing honest credible intervals and near-ideal calibration. Applied to the Fort Myers Hurricane Ian dataset, the dual approach reveals that while transfer learning excels at fast, high-F1 predictions, the Bayesian model delivers robustness and quantified uncertainty under extreme data imbalance—making it a powerful complement when engineering decisions demand both accuracy and confidence.

4 Conclusions

In adapting hurricane-induced fragility models to data-scarce regions, combining conventional transfer learning and hierarchical Bayesian transfer learning leverages the strengths of both: transfer learning rapidly improves classification accuracy—achieving high F1 scores with as few as ten local samples and gains from fine-tuned building features—while the hierarchical Bayesian model, although slower to converge, pools information across categories, yields well-calibrated posterior distributions with credible intervals, and remains robust under severe class imbalance. Thus, transfer learning is best suited for scenarios demanding fast, high-accuracy point estimates and rapid deployment, whereas the hierarchical Bayesian approach is preferable when quantified predictive uncertainty and calibrated confidence bounds are critical for risk-informed decision-making. Future work may extend these frameworks to other structural typologies and multi-hazard scenarios. Together, these methodologies offer a versatile toolkit for developing more accurate, region-specific fragility models and ultimately fostering more resilient coastal infrastructure planning.

5 Acknowledgment

The authors gratefully acknowledge support from the National Science Foundation under Award No. 2429680.

REFERENCES

[1] K. M. Crossett, “Population Trends Along the Coastal United States: 1980-2008”.

[2] B. Neumann, A. T. Vafeidis, J. Zimmermann, and R. J. Nicholls, "Future Coastal Population Growth and Exposure to Sea-Level Rise and Coastal Flooding - A Global Assessment," *PLoS ONE*, vol. 10, no. 3, p. e0118571, Mar. 2015, doi: 10.1371/journal.pone.0118571.

[3] P. J. Webster, G. J. Holland, J. A. Curry, and H.-R. Chang, "Changes in Tropical Cyclone Number, Duration, and Intensity in a Warming Environment," *Science*, vol. 309, no. 5742, pp. 1844–1846, Sep. 2005, doi: 10.1126/science.1116448.

[4] D. Lallemant, A. Kiremidjian, and H. Burton, "Statistical procedures for developing earthquake damage fragility curves," *Earthq Engng Struct Dyn*, vol. 44, no. 9, pp. 1373–1389, Jul. 2015, doi: 10.1002/eqe.2522.

[5] K. Porter, R. Kennedy, and R. Bachman, "Creating Fragility Functions for Performance-Based Earthquake Engineering," *Earthquake Spectra*, vol. 23, no. 2, pp. 471–489, May 2007, doi: 10.1193/1.2720892.

[6] H. Masoomi, J. W. Van De Lindt, M. R. Ameri, T. Q. Do, and B. M. Webb, "Combined Wind-Wave-Surge Hurricane-Induced Damage Prediction for Buildings," *J. Struct. Eng.*, vol. 145, no. 1, p. 04018227, Jan. 2019, doi: 10.1061/(ASCE)ST.1943-541X.0002241.

[7] A. Paleo-Torres *et al.*, "Vulnerability of Florida residential structures to hurricane induced coastal flood," *Engineering Structures*, vol. 220, p. 111004, Oct. 2020, doi: 10.1016/j.engstruct.2020.111004.

[8] O. M. Nofal, J. W. Van De Lindt, and T. Q. Do, "Multi-variate and single-variable flood fragility and loss approaches for buildings," *Reliability Engineering & System Safety*, vol. 202, p. 106971, Oct. 2020, doi: 10.1016/j.ress.2020.106971.

[9] C. C. Massarra, C. J. Friedland, B. D. Marx, and J. C. Dietrich, "Multihazard Hurricane Fragility Model for Wood Structure Homes Considering Hazard Parameters and Building Attributes Interaction," *Front. Built Environ.*, vol. 6, p. 147, Sep. 2020, doi: 10.3389/fbuil.2020.00147.

[10] X. Wang, R. K. Mazumder, B. Salarieh, A. M. Salman, A. Shafieezadeh, and Y. Li, "Machine Learning for Risk and Resilience Assessment in Structural Engineering: Progress and Future Trends," *J. Struct. Eng.*, vol. 148, no. 8, p. 03122003, Aug. 2022, doi: 10.1061/(ASCE)ST.1943-541X.0003392.

[11] H. Adeli and C. Yeh, "Perceptron Learning in Engineering Design," *Computer aided Civil Eng*, vol. 4, no. 4, pp. 247–256, Dec. 1989, doi: 10.1111/j.1467-8667.1989.tb00026.x.

[12] Y. Li, W. Hu, H. Dong, and X. Zhang, "Building Damage Detection from Post-Event Aerial Imagery Using Single Shot Multibox Detector," *Applied Sciences*, vol. 9, no. 6, p. 1128, Mar. 2019, doi: 10.3390/app9061128.

[13] L. Calton and Z. Wei, "Using Artificial Neural Network Models to Assess Hurricane Damage through Transfer Learning," *Applied Sciences*, vol. 12, no. 3, p. 1466, Jan. 2022, doi: 10.3390/app12031466.

[14] S. Kaur, S. Gupta, S. Singh, D. Koundal, and A. Zaguia, "Convolutional neural network based hurricane damage detection using satellite images," *Soft Comput*, vol. 26, no. 16, pp. 7831–7845, Aug. 2022, doi: 10.1007/s00500-022-06805-6.

[15] Haiyan Hao and Y. Wang, "Hurricane Damage Assessment with Multi-, Crowd-Sourced Image Data: A Case Study of Hurricane Irma in the City of Miami," 2020, doi: 10.13140/RG.2.2.35606.50245.

[16] F. Yuan and R. Liu, "Mining Social Media Data for Rapid Damage Assessment during Hurricane Matthew: Feasibility Study," *J. Comput. Civ. Eng.*, vol. 34, no. 3, p. 05020001, May 2020, doi: 10.1061/(ASCE)CP.1943-5487.0000877.

[17] L. Szczyrba, Y. Zhang, D. Pamukcu, D. I. Eroglu, and R. Weiss, "Quantifying the Role of Vulnerability in Hurricane Damage via a Machine Learning Case Study," *Nat. Hazards Rev.*, vol. 22, no. 3, p. 04021028, Aug. 2021, doi: 10.1061/(ASCE)NH.1527-6996.0000460.

[18] V. Wendler-Bosco and C. Nicholson, "Modeling the economic impact of incoming tropical cyclones using machine learning," *Nat Hazards*, vol. 110, no. 1, pp. 487–518, Jan. 2022, doi: 10.1007/s11069-021-04955-8.

[19] H. C. W. Van Verseveld, A. R. Van Dongeren, N. G. Plant, W. S. Jäger, and C. Den Heijer, "Modelling multi-hazard hurricane damages on an urbanized coast with a Bayesian Network approach," *Coastal Engineering*, vol. 103, pp. 1–14, Sep. 2015, doi: 10.1016/j.coastaleng.2015.05.006.

[20] S. Klepac, A. Subgranon, and M. Olabarrieta, "A case study and parametric analysis of predicting hurricane-induced building damage using data-driven machine learning approach," *Front. Built Environ.*, vol. 8, p. 1015804, Nov. 2022, doi: 10.3389/fbuil.2022.1015804.

[21] T. Q. Do, J. W. Van De Lindt, and D. T. Cox, "Hurricane Surge-Wave Building Fragility Methodology for Use in Damage, Loss, and Resilience Analysis," *J. Struct. Eng.*, vol. 146, no. 1, p. 04019177, Jan. 2020, doi: 10.1061/(ASCE)ST.1943-541X.0002472.

[22] S. A. Figueira, M. Amini, D. T. Cox, and A. R. Barbosa, "Methodology for Virtual Damage Assessment and First-Floor Elevation Estimation: Application to Fort Myers Beach, Florida and Hurricane Ian (2022)," *Nat. Hazards Rev.*, vol. 26, no. 2, p. 04025012, May 2025, doi: 10.1061/NHREFO.NHENG-2310.

[23] M. Amini, D. Cox, A. Barbosa, and S. Appleton Figueira, "An integrated Pre and Post Storm Dataset for Hurricane Ian (2022)." Designsafe-CI, 2025. doi: 10.17603/DS2-C1G8-QY41.

[24] C. Kaiser, C. N. Dawson, E. NIKIDIS, and J. G. Fleming, "ADCIRC/SWAN Hindcasts for Historical Storms 2003-2023." Designsafe-CI, 2023. doi: 10.17603/DS2-B5GH-CE94.